FIBERIZED SAGNAC INTERFEROMETER FOR ULTRASOUND MEASUREMENT

Pavel Fomitchov, Sridhar Krishnaswamy, and Jan D. Achenbach
Center for Quality Engineering and Failure Prevention
Northwestern University
Evanston, IL 60208

INTRODUCTION

Laser-based ultrasonics (LBU), i.e. the generation of ultrasound by laser illumination and the measurement of ultrasonic signals by laser interferometric techniques, has many advantages for applications to nondestructive evaluation (NDE). These include non-contact generation and detection, remote placement of equipment using fiber-optics, easy scanning, absolute displacement calibration, both broad band and narrow band signal generation, wide frequency band measurements, and applicability to curved surfaces. Both laser generation of ultrasound and the subsequent detection of the ultrasonic waves using a laser interferometry are areas of active research [1-6].

In earlier papers, the present authors have discussed an LBU system which employs a diffraction grating for illumination of a line-array to generate narrow-band surface waves and Lamb waves [4], and a fiberized heterodyne dual-probe laser interferometer to measure signals [3]. This paper reports progress toward the development of a robust low cost fiberized Sagnac laser interferometer suitable for field applications. Bowers first reported in reference [7] the use of a Sagnac-type interferometer for surface acoustic wave detection, and this work builds on that earlier effort . The primary advantage of the Sagnac interferometer is that it is exactly path matched and as such requires no heterodyning or static path compensation for sensor stabilization. The Sagnac interferometer described below is suitable for the measurement of ultrasonic surface waves arising from laser- or pzt-generated sources or from acoustic emissions. The laser-based ultrasonics (LBU) system can be used to detect and characterize discrete defects such as fatigue cracks as well as distributed regions of reduced material properties.

PRINCIPLE OF THE SAGNAC INTERFEROMETER

The fiberized Sagnac interferometer is shown in Figure 1. A linearly polarized laser beam is coupled into a single-mode fiber. This beam is split into two legs by a 2x2 coupler and these are in turn recoupled by a 2x1 coupler. One of the fiber legs contains a fiber phase modulator. The recoupled beams are then focused onto a test specimen through a grin lens focusing probe. The scattered light from the object is then collected by the grin lens probe, gets split along the two legs, and eventually reaches the photodetector as shown in the figure. All the fibers and couplers are polarization-maintaining to minimize polarization scrambling of the beams. We will call the central portion between the two couplers the Sagnac loop.

There are four paths that the light can travel from the laser to the specimen and back into the photodetector. Two of these will have returned by the same leg (leg 1 or leg 2) through which they entered (i.e. without going through the Sagnac loop). The other two are the one that enters leg 1 and returns by leg 2 (traveling the Sagnac loop clockwise) and the one that enters leg 2 and returns by leg 1 (traveling the Sagnac loop counter-clockwise).

Review of Progress in Quantitative Nondestructive Evaluation, Vol. 15
Edited by D.O. Thompson and D.E. Chimenti, Plenum Press, New York, 1996

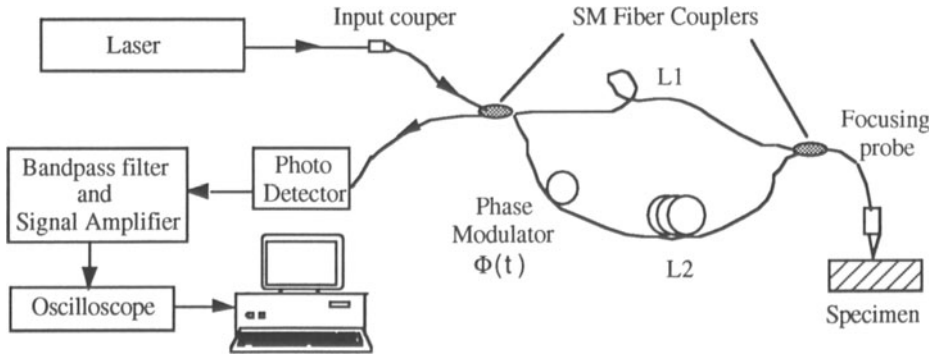

Figure 1: Schematic of the proposed interferometer.

By suitably choosing the path length difference along the two legs to be larger than the coherence length of the laser, it is possible to ensure that coherent interference will occur only between the clockwise and counter-clockwise beams. The advantage of the Sagnac interferometer over Michelson is immediately apparent. This interferometer is a truly path-matched setup and as such will be unaffected by low frequency thermal fluctuations and vibratory noise. The need for electronic demodulation of the heterodyne Michelson interferometer signal or for active stabilization of the path-stabilized homodyne Michelson interferometer is obviated in the case of the proposed device. The electric field at the photodetector for the light that enters and returns along leg 1 only is then given by :

$$e_{11}(t) = E_0 \exp\left[-i\left\{2kL_1 + 2k\, u\left(t-\frac{nL_1}{c}\right)\right\}\right]; \qquad (1)$$

for the light that enters and returns along leg 2 only :

$$e_{22}(t) = E_0 \exp\left[-i\left\{2kL_2 + \phi(t) + \phi\left(t-\frac{2nL_2}{c}\right) + 2k\, u\left(t-\frac{nL_2}{c}\right)\right\}\right]; \qquad (2)$$

for the light that enters along leg 1 and returns along leg 2 traversing the Sagnac loop clockwise :

$$e_{12}(t) = E_0 \exp\left[-i\left\{kL + \phi(t) + 2k\, u\left(t-\frac{nL_2}{c}\right)\right\}\right]; \qquad (3)$$

and for the light that enters along leg 2 and returns along leg 1 traversing the Sagnac loop counter-clockwise :

$$e_{21}(t) = E_0 \exp\left[-i\left\{kL + \phi\left(t-\frac{nL}{c}\right) + 2k\, u\left(t-\frac{nL_1}{c}\right)\right\}\right]. \qquad (4)$$

Here $k = 2\pi/\lambda$ is the laser wave number; λ is the laser light frequency; c is the speed of light in free space and n the refractive index of the fiber core; $\phi(t)$ is the phase modulation function; and $u(t)$ is the ultrasonic displacement to be detected. L_1 and L_2 are the lengths of the two interferometer legs; $L=L_1+L_2$ is the total length of the Sagnac loop. Note that the ultrasonic signal sensed by the various beams as well as their phase modulation come from different times because of the difference in the lengths of the two legs. By appropriate choice of the laser source and the lengths of the leg L_1 and L_2, coherent interference will occur only between the clockwise and counter-clockwise beams, and the resulting interference intensity measured at the photodetector is:

$$I(t) = E_0^2\left\{1 + \frac{1}{2}\cos\left[\phi(t) - \phi\left(t-\frac{nL}{c}\right) + 2ku\left(t-\frac{nL_2}{c}\right) - 2ku\left(t-\frac{nL_1}{c}\right)\right]\right\}. \qquad (5)$$

For a harmonic ultrasonic signal: $u(t) = A \cos \omega_a t$, where A is the ultrasonic displacement amplitude, and ω_a the frequency, the resulting intensity becomes:

$$I(t) = E_0^2 \left\{ 1 + \frac{1}{2} \cos \left[\phi(t) - \phi\left(t - \frac{nL}{c}\right) + 4kA \sin\left[\frac{\omega_a n \Delta L}{2c}\right] \sin\left[\omega_a \left(t - \frac{nL}{2c}\right)\right]\right]\right\}, \qquad (6)$$

where $\Delta L = L_2 - L_1$ is the loop length difference.

Since ultrasonic displacements are a fraction of the laser wavelength, ie, $kA << 1$, it is important to ensure in the above equation that $\sin\left[\frac{\omega_a n \Delta L}{2c}\right] = 1$. This can be achieved by setting the loop length difference appropriately for a given ultrasonic frequency, to provide a time delay $\tau = \frac{n \Delta L}{c}$ between clockwise and counter-clockwise beams equal to one half the period of the ultrasonic wave. Furthermore, the best sensitivity for the interferometer is obtained if the phase-modulator can be used to put the interferometer at quadrature, i.e. if the clockwise and counter-clockwise beams are made to be $\pi/2$ out of phase:

$$\phi(t) - \phi\left(t - \frac{nL}{c}\right) = \frac{\pi}{2} . \qquad (7)$$

This condition can be achieved at essentially all times, if a suitable ramp (actually saw-tooth) function is used to drive the phase modulator as shown in Fig. 2.

With the system optimised as indicated above, the photodetector output after suitable high pass filtering becomes:

$$I(t) \approx 4kA \sin\left\{w_a\left(t - \frac{nL}{2c}\right)\right\} . \qquad (8)$$

The above shows that the interferometer signal is proportional to the ultrasonic amplitude, but is phase shifted by an amount that depends on the frequency. For this reason and due to the fact that the loop length difference can be optimized only for a given ultrasonic frequency, it is clear that the gain of simplicity of this interferometer over heterodyne or path-stabilized systems comes with the restriction that this type of an interferometer is best used for narrowband signals. This is not really a serious drawback since there are many instances when narrowband generation and detection are desirable [4].

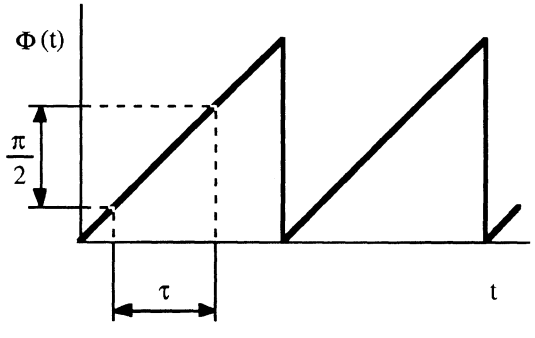

Fig. 2: The saw-tooth phase modulation function.

RESULTS AND DISCUSSION

Partially as well as fully fiberized versions of the above-described Sagnac ultrasound detectors were configured. The laser sources used were a multimode 5 mW HeNe laser and a 30 mW diode laser at center wavelength 633 nm and 690 nm respectively. The fiber phase modulator used was based on piezoelectric stretching of a loop of fiber. To ensure that the phase shift between both the clockwise and the counter-clockwise beams is constant with time, the ultrasound toneburst generation is synchronized with the phase modulator driving signal. All the fibers and the directional couplers were polarization-preserving systems. The loop length difference was kept at 20 m which is near optimal for 5 MHz ultrasonic signals. As discussed in reference [6], a GRIN lens is glued to the end of the probing fiber to focus the light beam onto the surface of the specimen and also to collect the return light back into the Sagnac device. At the present time, it is essential to have a relatively reflective specimen surface in order to collect sufficient amount of light from the specimen. In this aspect, the Sagnac interferometer suffers from the same drawback as the heterodyne Michelson-interferometer. Methods to overcome this limitation include having a sufficiently powerful laser source or utilizing an automated search procedure to locate bright speckles.

Detection of Surface Acoustic Waves

To verify that the Sagnac interferometer performs as expected, surface acoustic waves in an aluminum block were measured. A piezoelectric transducer, with a center frequency of 5 MHz and mounted on a surface wave generating wedge, is employed to generate an ultrasound signal as shown schematically in fig. 3. A function generator and power amplifier combination was used to generate the 5MHz tonebursts.

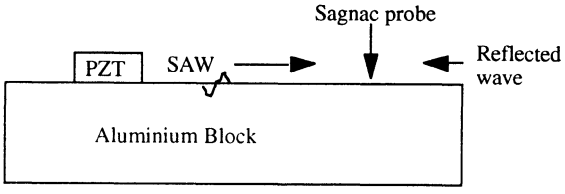

Fig. 3: Setup for surface acoustic wave detection.

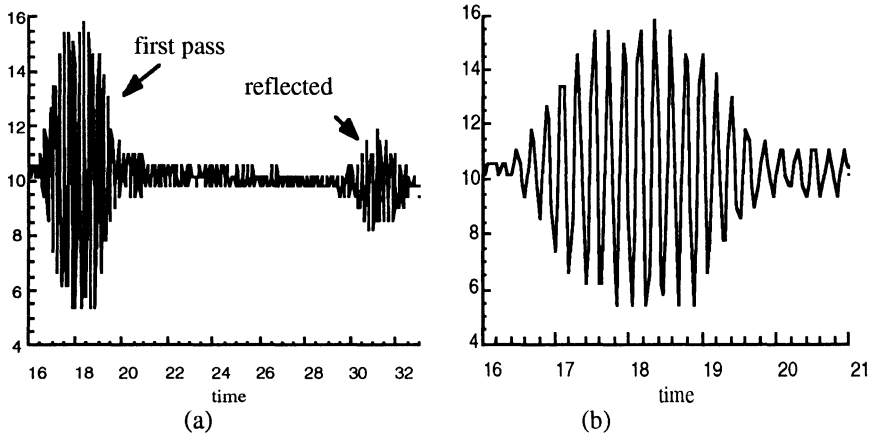

Fig. 4: (a) First pass and reflected wave and (b) magnified first pass toneburst.

The Sagnac probe picks up both the first pass signal as well as the signal reflected from the end of the specimen as shown in fig. 4a; figure 4b., is an expanded view of the first pass signal detected by the Sagnac interferometer. The measured wave speed of 2900 m/s is consistent with a Rayleigh wave speed of 2910 m/s for Aluminum [8].

Detection of cracks in simulated aircraft panels

The Sagnac interferometer has also been applied to the detection of simulated cracks emanating from rivet holes. The specimen is made of two aluminum alloy plates, 2 mm thick, that are riveted together as shown in fig. 5. Two EDM notches are made to emanate from the countersunk rivet hole in the top plate before the two plates are riveted together. The same piezoelectric transducer arrangement described above was used to generate 5MHz tonebursts. The transducer is aligned with the center axis of the rivet. Because the thickness of the plate is comparable to the acoustic wavelength, Lamb waves are generated. Since the transducer generation cannot really be considered a plane wave, we scanned two lines along the path of the ultrasonic beam as shown in fig.5. The first line bB was ahead of the rivet-crack, and the second line aA was behind the crack.

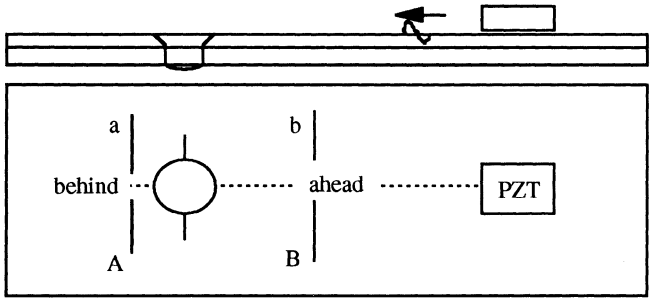

Fig. 5: Rivet / crack specimen.

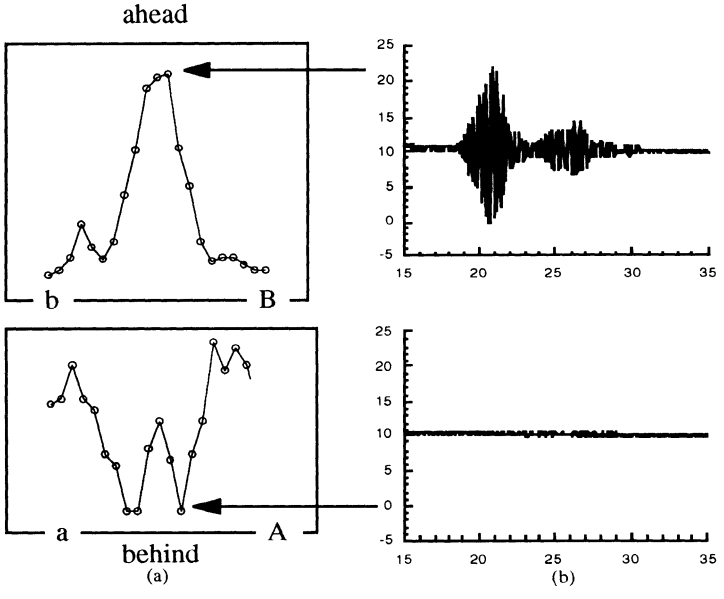

Fig. 6: (a) Amplitude of transmitted signal at different scanning locations along bB ahead and aA ahead of the rivet / crack; and (b) representative ultrasonic signal ahead and behind the rivet / crack.

The corresponding signal amplitudes for various scanning points along these two lines are shown in fig. 6a. Representative traces of the actual ultrasonic signal are shown in fig. 6b. It is clear from the trace along aA that the crack shadows the ultrasonic signal resulting in total loss of the detected signal at some locations. Two interesting points can be noted: (i) there is a certain amount of signal that getstransmitted through the center of the rivet and this shows up as a higher amplitude signal at the center in trace aA; and (ii) at certain scanning locations along bB ahead of the rivet-crack, a secondary signal due to reflection from the rivet/crack can be seen after the strong first pass signal. All these findings were consistent with previous results we have obtained on the same specimen but using a dual-probe heterodyne Michelson interferometer [6].

CONCLUSION

A fiberized Sagnac interferometer has been configured to measure ultrasound. The interferometer is a truly path-matched device, and it is a more robust alternative to the heterodyne or path-stabilized Michelson interferometer. The device will form part of a complete laser-based ultrasonic NDE system. At present, we have used the system to detect Rayleigh waves and to measure reflection and transmission of the ultrasonic wave by rivet/cracks in rivetted plates.

ACKNOWLEDGEMENTS

This material is based upon work performed at Northwestern University for the FAA Center for Aviation Systems Reliability operated by Iowa State University and supported by the Federal Aviation Administration under Grant No. 93-G-018.

REFERENCES

1. C.B. Scruby and L.E. Drain, *Laser Ultrasonics* (Adam Hilger, New York, 1990).
2. J.B. Spicer and J.W.Wagner, *NDE. of Materials,* edited by P. Holler, et al, (Springer-Verlag, New York, 1989), p. 691-698.
3. J. Huang and J. D. Achenbach, J. Acoust. Soc. Am., 90(3), p. 1269, (1991).
4. J. Huang, S. Krishnaswamy and J. D. Achenbach, J. Acoust. Soc. Am., vol. 92(5), p. 2527-2531, (1992).
5. J. Huang, S. Krishnaswamy and J. D. Achenbach, *Rev. Prog. Quantitative NDE,* vol. 13A, edited by D.O.Thompson and D.E.Chimenti, (Plenum Press, New York, 1993), p. 485-492.
6. J. Huang, S. Krishnaswamy and J. D. Achenbach, *Rev. Prog. Quantitative NDE,* vol. 12A, edited by D.O.Thompson and D.E.Chimenti, (Plenum Press, New York, 1992), p. 503-510.
7. J.E. Bowers, Applied Physics Letters, vol. 41(3), 231 (1982).
8. J. Krautkramer, H. Krautkramer, *Ultrasonic Testing of Materials* (Springer - Verlag, Berlin, 1990).